

SOME 3-THIAZINONYL-BICYCLO [4.2.0] OCTENE-CARBOXYLATE DERIVATIVES AS ENVIRONMENTALLY-FRIENDLY CORROSION INHIBITORS OF STAINLESS STEEL TYPE 304 IN 1.0M HCL SOLUTION

A.S. Fouda^{*}, H.A. Mostafa, W.M. Abo-Elmeaty and H.M. El-Abbasy
Department of Chemistry, Faculty of Science, El-Mansoura University,
El-Mansoura- 35516, Egypt. E-mail: asfouda@mans.edu.eg

(Received: 1/2/2009)

ABSTRACT

The effect of 3-thiazinonyl-bicyclo [4.2.0] octene-carboxylate derivatives on the corrosion behavior of stainless steel type 304 in 1.0 M HCl solution has been investigated using weight loss, potentiodynamic polarization and electrochemical impedance spectroscopy (EIS) techniques. The inhibition efficiency increased with increase in inhibitor concentration but decreased with increase in temperature. The thermodynamic functions of corrosion and adsorption processes were evaluated. The potentiodynamic polarization measurements indicated that the inhibitors are of mixed type. The adsorption of these inhibitors was found to obey Langmuir's adsorption isotherm. Synergism between iodide ion and inhibitors was proposed. The inhibitive action was satisfactorily explained by using both thermodynamic and kinetic models. The results obtained from the three different techniques were in good agreement.

Keywords. Corrosion, HCl, 3-thiazinonyl-bicyclo [4.2.0] octene-carboxylate derivatives, stainless steel type 304.

1. INTRODUCTION

Stainless steel type 304 has found wide applications in variety of industries. It is covered with a highly protective film of chromium oxide and is resistant to corrosion in many aggressive environments. It is possible to reduce the corrosion rate to safe level by adding

inhibitors. Organic compounds and their derivatives were used successfully as inhibitors for different types of steels and were studied extensively through the last century. Recently, interest is still growing for exploiting other inhibitors for the corrosion of stainless steels [Szypowski (2002)]. Several organic molecules containing sulfur, oxygen and nitrogen hetero-atoms were suggested as inhibitors for steel in acidic medium [Quraishi *et al.*, (2003); Elachouri *et al.*, (1995); Merari *et al.*, (1998); Bentiss *et al.*, (2000); Elkadi *et al.*, (2000); Walker (1975) and Bentiss *et al.*, (1999)]. The inhibition mechanism for this class of inhibitors is mainly based on adsorption [El-Kanouni *et al.*, (1996)].

The present investigation aimed to study the effect of three 3-thiazinonyl-bicyclo[4.2.0] octene-carboxylate derivatives as environmentally-friendly corrosion inhibitors for the corrosion of stainless steel type 304 in 1.0 M HCl. Also, the relationship between calculated quantum chemical parameters and experimental inhibition efficiencies of the inhibitors was discussed.

2. EXPERIMENTAL METHODS

2.1. Materials

The experiments were performed with stainless steel type 304 specimens in the form of rods and sheets with the following composition: C = 0.1%, Mn 0.5%, P = 0.025%, S = 0.025%, Fe remainder.

2.2. Solutions

The aggressive solutions used were made of AR grade HCl. Appropriate concentrations of acid were prepared using distilled water. 10^{-3} mol l^{-1} stock solutions from the investigated compounds were prepared by dissolving the appropriate weights of the used chemically pure solid compounds in distilled water.

2.3. Weight loss method

Three parallel stainless steel sheets of 2 x 2 x 0.2 cm were abraded with emery paper up to 1200 grit, and then washed with distilled water and acetone. After weighing accurately, the specimens were immersed in 100 ml beaker, which contained 100 ml HCl with and without addition of different concentrations of inhibitors. All the aggressive acid solutions were open to air. After 6 h, the specimens were

taken out, washed, dried, and weighed accurately. The average weight loss of the three parallel stainless steel sheets could be obtained. Then the tests were prepared at different temperatures. The inhibition efficiency (IE) and the degree of surface coverage (θ) of investigated inhibitors on the corrosion of stainless steel were calculated as follows [Talati & Modi (1986)]:

$$IE\% = [(W_0 - W) / W_0] \times 100 \quad (1)$$

$$\theta = [(W_0 - W) / W_0] \quad (2)$$

where W_0 and W are the values of the average weight loss without and with addition of the inhibitor, respectively.

2.4 Potentiodynamic polarization measurements

Polarization experiments were carried out in a conventional three-electrode cell with a platinum counter electrode and a saturated calomel electrode coupled to a fine Luggin capillary as the reference electrode. The working electrode was in the form of a square cut from stainless steel sheet (1cm x 1cm) embedded in epoxy resin of polytetrafluoroethylene so that the flat surface was the only surface in the electrode. Before polarization scanning, working electrode was immersed in the test electrolyte of 100 ml in volume for 20 min. until steady state and the open circuit potential (OCP) was attained which was taken as E_{OC} . All potentiodynamic measurements were carried out with a Gamry framework instruments (version 3.20), controlled by a computer which also recorded and stored the data. All experiments were carried out at $25 \pm 1^\circ\text{C}$ using Lab companion circulator thermostat model CW-05GL and solutions were not deaerated. For polarization measurements potential from -300 to 100 mV (relative to open circuit potential, E_{OC}) was applied while potential from -500 to 700 mV (relative to reference electrode potential, E_{ref}) was applied in case of pitting measurements. IE% and the degree of surface coverage (θ) were defined as:

$$IE\% = [(i_{corr} - i_{corr(inh)}) / i_{corr}] \times 100 \quad (3)$$

$$\theta = [(i_{corr} - i_{corr(inh)}) / i_{corr}] \quad (4)$$

Where i_{corr} and $i_{corr(inh)}$ are the uninhibited and inhibited corrosion current density values, respectively, determined by extrapolation of Tafel lines to the corrosion potential.

2.5. Electrochemical impedance spectroscopy method

The EIS spectra were recorded at open circuit potential (OCP) after immersion the electrode for 10 minutes in the test solution. The AC

signal was 5 mV peak to peak and the frequency range studied was between 100 kHz and 0.2 Hz. All Electrochemical impedance experiments were carried out using Potentiostat/ Galvanostat/Zra analyzer (Gamry PCI300/4). A personal computer with EIS300 software and Echem Analyst 5.21 was used for data fitting and calculating.

The inhibition efficiency (IE%) and the surface coverage (θ) of the used inhibitors obtained from the impedance measurements can be calculated by applying the following relations:

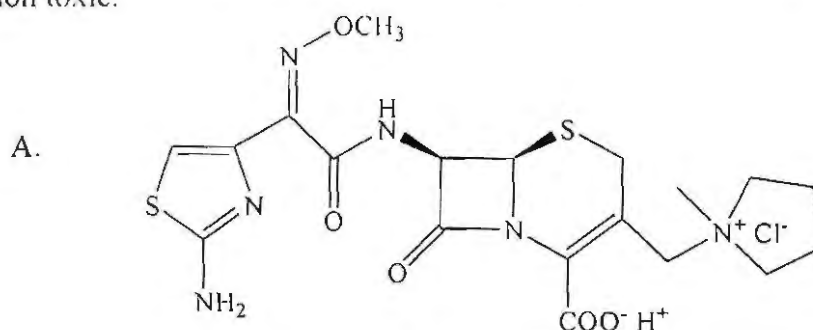
$$\%IE = \left(1 - \frac{R_{ct}^0}{R_{ct}} \right) \times 100 \quad (5)$$

$$\theta = \left(1 - \frac{R_{ct}^0}{R_{ct}} \right) \quad (6)$$

where R_{ct}^0 and R_{ct} are the charge transfer resistance in the absence and presence of inhibitor, respectively.

2.6. Inhibitors

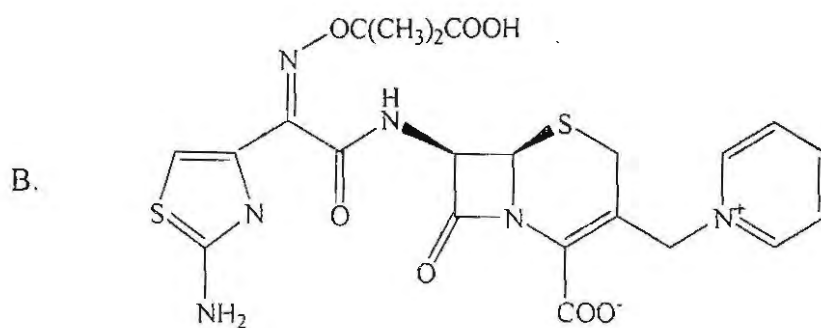
The following three 3-thiazinonyl-bicyclo[4.2.0] octene-carboxylate derivatives were used as inhibitors for the corrosion of stainless steel type 304 in 1M HCl. These derivatives were selected because: availability, with large molecular size, easily soluble in water and non toxic.



(6R, 7R, Z)-7-(2-(2-aminothiazol-4-yl)-2-(methoxyimino)acetamido)-3-(1-methyl pyrrolidinium-1-yl)methyl)-8-oxo-5-thia-1-azabicyclo[4.2.0]oct-2-ene-2-carboxylate

(Produced by Bristol-Myers Squibb Egypt Company, Egypt)

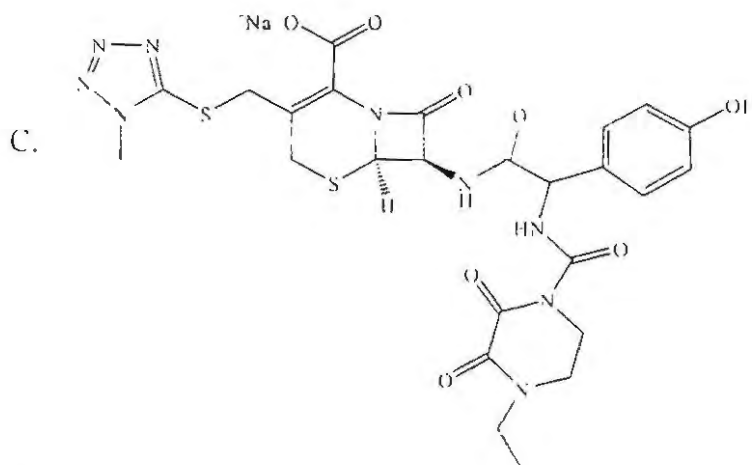
Chemical Formula: $C_{19}H_{25}ClN_6O_5S_2$ Molecular Weight: 517.02



(6R,7R, Z)-7-(2-(2-aminothiazol-4-yl)-2-(2-carboxypropan-2-yl)oxyimino) acetamido)-8-oxo-3-(pyridinium-1-ylmethyl)-5-thia-1-azabicyclo[4.2.0]oct-2-ene-2-carboxylate

(Produced by Glaxo Smithkline Company)

Chemical Formula: $C_{22}H_{22}N_6O_7S_2$ Molecular Weight: 546.58



(6R, 7R, Z)-7-{|2-[(4-ethyl-2,3-dioxo-piperazine-1-carbonyl)amino]-2-(4-hydroxyphenyl)acetyl} amino}-3-[(1-methyltetrazol-5-yl)sulfanylmethyl]-8-oxo-5-thia-1-aza-bicyclo[4.2.0]oct-2-ene-2-carboxylic acid

(Produced by Pharco Pharmaceutical Company, Egypt)

Chemical Formula: $C_{25}H_{26}N_9NaO_8S_2$ Molecular Weight: 667.65

3. RESULTS AND DISCUSSION

3.1. Weight loss measurements

The weight loss of stainless steel type 304 specimen in 1.0 M HCl solution, with and without different concentrations from the investigated inhibitors, was determined after 6 h of immersion at 25°C. Fig.1 represents this for compound (C) as an example. Similar curves were obtained for other inhibitors (not shown). Obtained values of IE% are given in Table (1). The presence of inhibitors reduces the corrosion rate of steel in HCl.

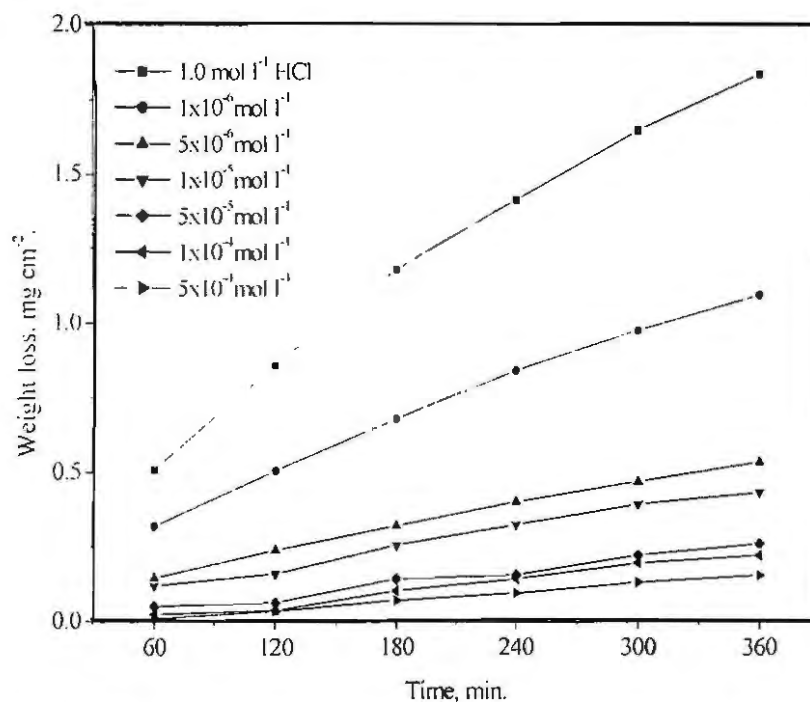


Fig.1. Weight loss- time curves for the corrosion of stainless steel type 304 in 1.0 mol l⁻¹ HCl in absence and presence of different concentrations of inhibitor (C) at 25°C.

3.1.1- Adsorption isotherm

One of the most convenient ways of expressing adsorption quantitatively is by deriving the adsorption isotherm that characterizes the metal/inhibitor/ environment system [Szklarska-Smiałowska (1991)] various adsorption isotherms were applied to fit θ values but the best was found to obey Langmuir adsorption isotherm [Langmuir & Amer (1947)] which may be expressed by:

$$\frac{C}{\theta} = \frac{1}{K} + C \quad (7)$$

where C is inhibitor concentration and K is equilibrium constant of adsorption (see Fig.2).

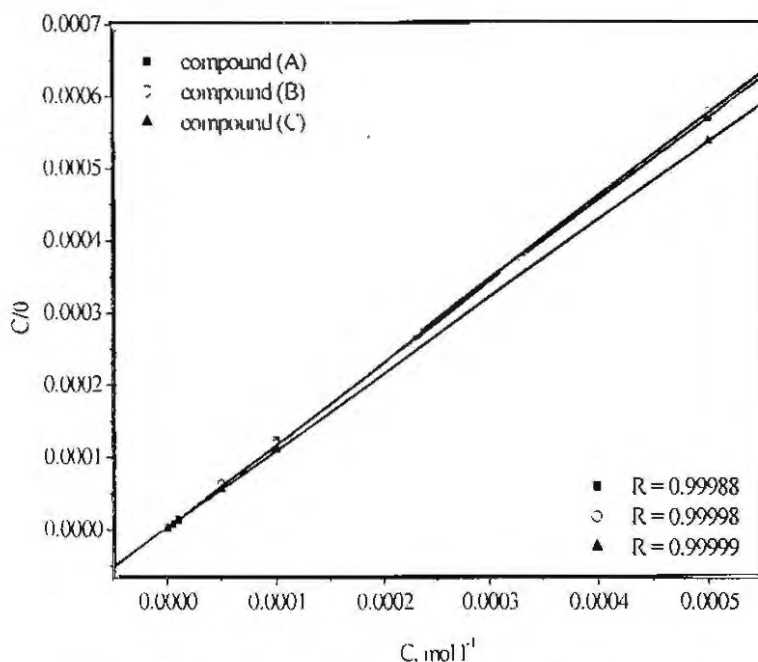


Fig. 2. Langmuir adsorption isotherm plotted as (C/θ) vs C of inhibitors A, B and C for corrosion of stainless steel type 304 in 1.0 mol l^{-1} HCl solution at 25°C .

It is well known that the standard adsorption free energy ($\Delta G^\circ_{\text{ads}}$) is related to equilibrium constant of adsorption (K) and $\Delta G^\circ_{\text{ads}}$ can be calculated by the following equation [Khamis (1990)].

$$K = 1/55.5 \exp [-\Delta G^\circ_{\text{ads}}/RT] \quad (8)$$

Fig. 2 represents the plot of (C/θ) against C for all investigated compounds. As can be seen from Fig. 2, the Langmuir isotherm is the best one which explains the experimental results. Also, it is found that the kinetic-thermodynamic model of El-Awady et al [El-Awady & Ahmed (1985)].

$$\log (\theta/ 1-\theta) = \log k' + y \log C \quad (9)$$

is valid to operate the present adsorption data. $K = K' (1/y)$, K' is constant and $1/y$ is the number of the surface active sites occupied by one inhibitor

molecule and C is the bulk concentration of the inhibitor. Plotting $\log(\theta/1-\theta)$ against $\log C$ for the compounds is given in Fig. 3. where straight-line relationships were obtained suggesting the validity of this model for the studied case. A plot of $\log(\theta/1-\theta)$ vs. $1/T$ at constant additives concentration ($5 \times 10^{-5} \text{ mol l}^{-1}$) (Fig. 4) gives straight lines according to the following equation:

$$\log \theta / 1-\theta = \log A + \log C - (Q/2.303RT) \quad (10)$$

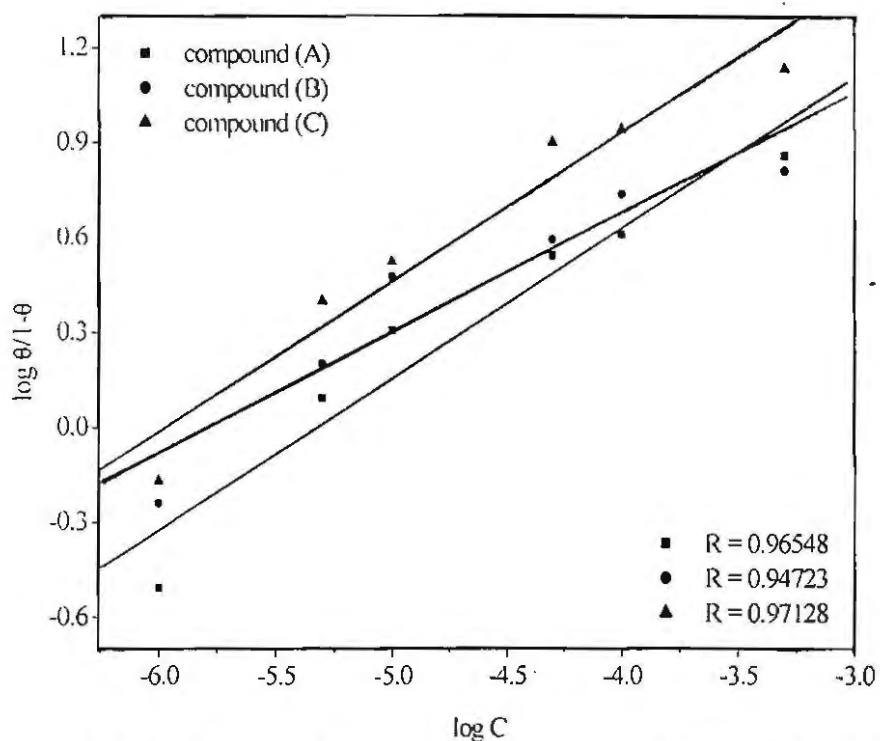


Fig. 3. El Awady et al model plotted as $\log(\theta/1-\theta)$ vs $\log C$ of inhibitors A, B and C for corrosion of stainless steel type 304 in 1.0 mol l^{-1} HCl solution at 25°C .

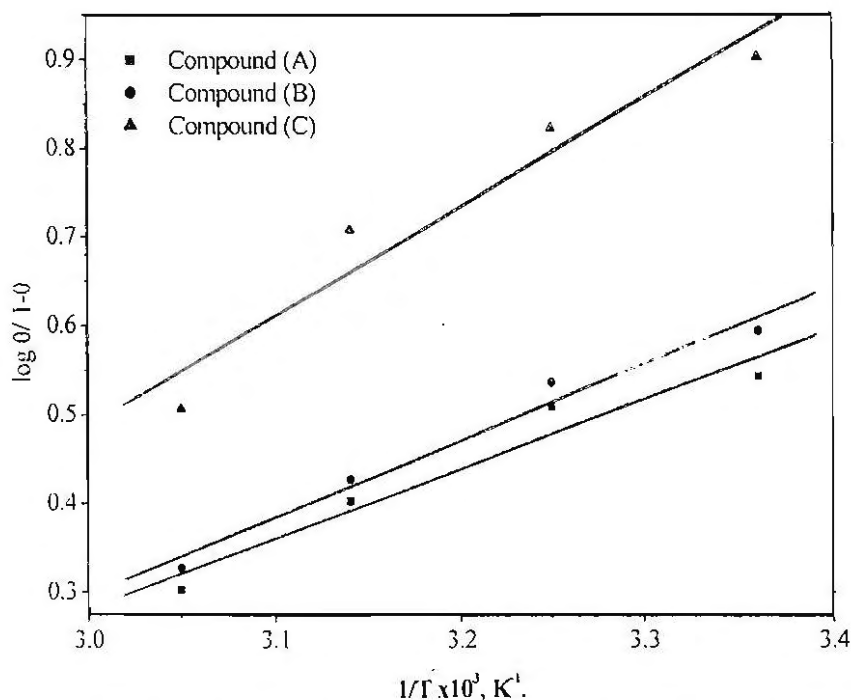


Fig. 4. Plots of $\log(\theta/(1-\theta))$ vs. $1/T$ for 5×10^{-5} mol l^{-1} of inhibitors A, B and C for corrosion of stainless steel type 304 in 1.0 mol l^{-1} HCl solution at 25°C.

The Q values were obtained from the slopes of these lines. The values of K and ΔG_{ads}° calculated by Langmuir isotherm and $1/y$, K and ΔG_{ads}° calculated by the kinetic model and the values of Q are given in Table (1). The negative values of ΔG_{ads}° suggest that the adsorption of inhibitors molecules onto steel surface is a spontaneous process. The magnitude of adsorption heat reaches the magnitude of chemical reaction heat, which is the result of the transference of electron from donating atoms in the inhibitor molecule to the d-orbital of the iron atom. The negative values of Q show that, the process of adsorption is exothermal. It is noting that the value of $1/y$ is more than unity. This means that the given inhibitor molecules will form monolayer on the steel surface. In general the values of ΔG_{ads}° obtained from El- Awady et al et model are comparable with those obtained from Langmuir isotherms.

Table (1): Binding constant (K), free energy of adsorption (ΔG_{ads}) and number of active sites ($1/y$) and for adsorption of inhibitors A, B and C and heat of adsorption (Q) of 5×10^{-5} mol l⁻¹ on stainless steel type 304 surface in 1.0 mol l⁻¹ HCl at 25°C.

Inhibitor	Kinetic model			Langmuir isotherm		-Q (kJ mol ⁻¹)
	1/y	K	$-\Delta G_{ads}$ (kJ mol ⁻¹)	K	$-\Delta G_{ads}$ (kJ mol ⁻¹)	
A	2.096	207556	40.291	177069	39.898	15.034
B	2.624	600667	42.925	353518	41.611	16.565
C	2.111	922377	43.988	410433	41.981	23.608

3.1.2- Kinetic parameters

The corrosion of stainless steel type 304 in 1.0 mol l⁻¹ HCl in absence and presence of different concentrations of the investigated inhibitors (ca. 1.0×10^{-6} to 5×10^{-4} mol l⁻¹) at temperatures range (25–55°C) was studied using weight loss method. The percentage inhibition efficiency (%IE) at each inhibitor concentration can be calculated using equation (1). The inhibition efficiency values at different temperatures were tabulated in Table (2). The obtained data reveal that the extent of the inhibition efficiency increases with the concentration of the inhibitors and decreases with increasing temperature. These types of inhibitors retard the corrosion process at ordinary temperature [Putilova *et al.*, (1960)] whereas the inhibition is considerably decreased at elevated temperature. The increasing of the corrosion rate with increasing the temperature is suggestive of physical adsorption of the used inhibitors on stainless steel type 304 surface.

Table (2): Effect of temperature on the inhibition efficiencies of different concentrations of inhibitors A, B and C for the corrosion of stainless steel type 304 in 1.0 mol l⁻¹ HCl.

Temp. T, °C	Inhibitor	IE%					
		[Inhibitor], M					
		1x10 ⁻⁶	5x10 ⁻⁶	1x10 ⁻⁵	5x10 ⁻⁵	1x10 ⁻⁴	5x10 ⁻⁴
25°C	A	23.8	55.4	67.0	77.7	80.3	87.9
	B	36.6	61.4	75.0	79.6	84.5	86.6
	C	40.5	75.5	77.0	88.8	89.8	93.2
35°C	A	-	53.3	59.0	76.3	78.1	87.8
	B	-	56.6	70.5	77.4	79.3	86.9
	C	-	68.6	75.1	86.9	88.9	93.5
45°C	A	-	35.2	51.8	71.6	73.5	85.4
	B	-	39.9	58.5	72.8	76.9	84.4
	C	-	51.2	64.2	83.6	86.3	90.8
55°C	A	-	28.7	42.5	66.7	68.7	83.5
	B	-	33.0	46.7	68.0	72.9	82.6
	C	-	29.3	44.3	76.2	83.4	91.9

The activation energy of the corrosion process can be calculated using Arrhenius-type equation:

$$k = A \exp(-E_a^*/RT) \quad (11)$$

where k is the corrosion rate, A is the pre-exponential factor, E_a^* is the apparent activation energy, R is the universal gas constant and T is the absolute temperature. The apparent activation energy at 5×10^{-5} mol l⁻¹ from the investigated inhibitors was calculated by linear regression between $\ln k$ and $(1/T)$ [Fig. 5]. The energy of activation for the compounds and the values of the thermodynamic parameter for the dissolution of stainless steel type 304 in 1.0 mol l⁻¹ HCl are listed in Table (3). Free energy of activation (ΔG^*) were calculated by applying the transition state equation [Laque & Gapson (1963)]

Table (3): Activation energy and thermodynamic activation parameters for dissolution of stainless steel type 304 in 1.0 mol l⁻¹ HCl in absence and presence of 5x10⁻⁵ mol l⁻¹ of inhibitors A, B and C at different temperatures.

Inhibitors	Thermodynamic activation parameters	Temperature. °C			
		25	35	45	55
1 M HCl	E _a [*] (kJ mol ⁻¹)	44.3			
	ΔG [*] (kJ mol ⁻¹)	85.7	87.1	88.8	90.0
	ΔH [*] (kJ mol ⁻¹)	41.8	41.8	41.7	41.6
	-ΔS [*] (J mol ⁻¹ K ⁻¹)	147.2	147.2	148.1	147.4
A	E _a [*] (kJ mol ⁻¹)	55.2			
	ΔG [*] (kJ mol ⁻¹)	89.4	90.8	92.1	93.0
	ΔH [*] (kJ mol ⁻¹)	52.8	52.7	52.6	52.5
	-ΔS [*] (J mol ⁻¹ K ⁻¹)	123.1	123.7	124.3	123.3
B	E _a [*] (kJ mol ⁻¹)	56.6			
	ΔG [*] (kJ mol ⁻¹)	89.7	90.9	92.2	93.2
	ΔH [*] (kJ mol ⁻¹)	54.1	54.0	54.0	53.9
	-ΔS [*] (J mol ⁻¹ K ⁻¹)	119.2	119.7	120.3	119.5
C	E _a [*] (kJ mol ⁻¹)	64.0			
	ΔG [*] (kJ mol ⁻¹)	91.1	92.3	93.6	93.9
	ΔH [*] (kJ mol ⁻¹)	61.5	61.4	61.4	61.3
	-ΔS [*] (J mol ⁻¹ K ⁻¹)	99.4	100.2	101.3	99.4

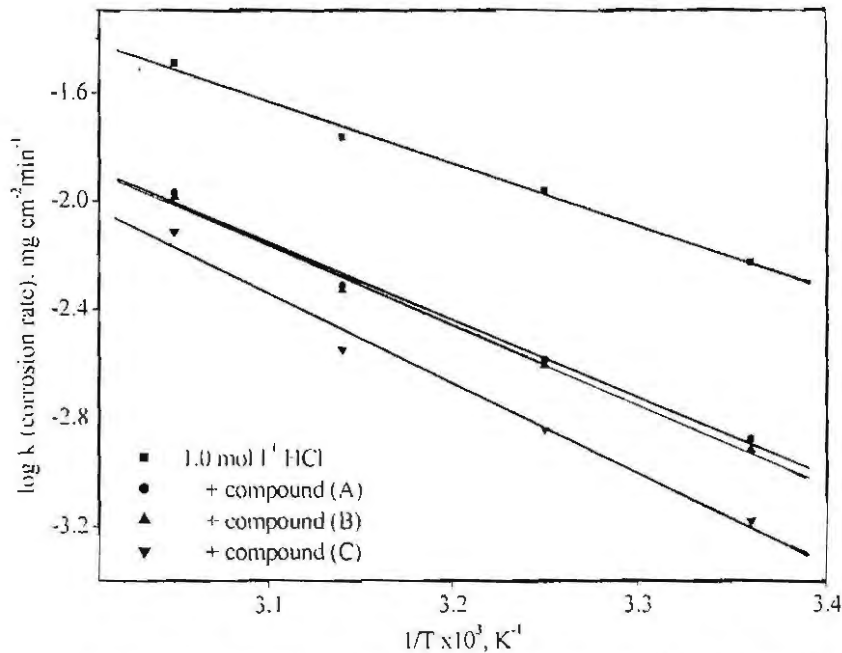


Fig. 5. Arrhenius plots ($\log K$ vs $1/T$) for stainless steel type 304 in 1.0 mol l^{-1} HCl in absence and presence of $5 \times 10^{-5} \text{ mol l}^{-1}$ of inhibitors A, B and C.

$$\Delta G^* = RT \left[\ln \frac{KT}{h} - \ln(\text{corrosion rate}) \right] \quad (12)$$

where, h is Planck's constant, K is Boltzman's constant, R is gas constant and T is absolute temperature. The enthalpy of activation (ΔH^*) and the entropy of activation (ΔS^*) were calculated by applying the following equations [El-Awady & Ahmed (1985)]

$$\Delta H^* = E_a^* - RT \quad (13)$$

$$\Delta S^* = \frac{\Delta H^* - \Delta G^*}{T} \quad (14)$$

The activation energy is higher in the presence of additives than in their absence. Similar results were obtained by other authors [E.Khamis (1990); Zhao & Mu (1999); Fouda *et al.*, (2005); Fouda *et al.*, (2009) and Riggs & Hurd (1967)]. The higher values of E_a^* are good evidence for the strong adsorption of 3-thiazinonyl-bicyclo[4.2.0] octene-carboxylate derivatives on the steel surface. The values of (ΔH^*) are positive and high in the presence of the inhibitors over that of the

uninhibited solution. This implies that energy barrier of the corrosion reaction in the presence of the investigated inhibitors increases. On the other hand ΔS^\ddagger values are lower and have negative values in presence of the inhibitors. this means that addition of these compounds cause a decrease in the disordering in going from reactants to the activated complexes [Riggs & Iurd (1967) and Gomma & Wahdan (1995)].

3.2. Potentiodynamic polarization measurements

Fig. 6 shows potentiodynamic polarization curves of stainless steel type 304 without and with different concentrations of compound (C) at 25°C as an example. Similar curves were obtained for other compounds.

The obtained electrochemical parameters; cathodic and anodic Tafel slopes (β_c and β_a , respectively), open circuit potential (E_{OC}), corrosion potential (E_{corr}), corrosion current density (i_{corr}), corrosion rate (C.R.) and polarization resistance (R_p) were obtained and listed in Table 4. The degree of surface coverage: θ at constant potential is given by the following relation [Ammar & Darwish (1967) and Fisher (1960)]

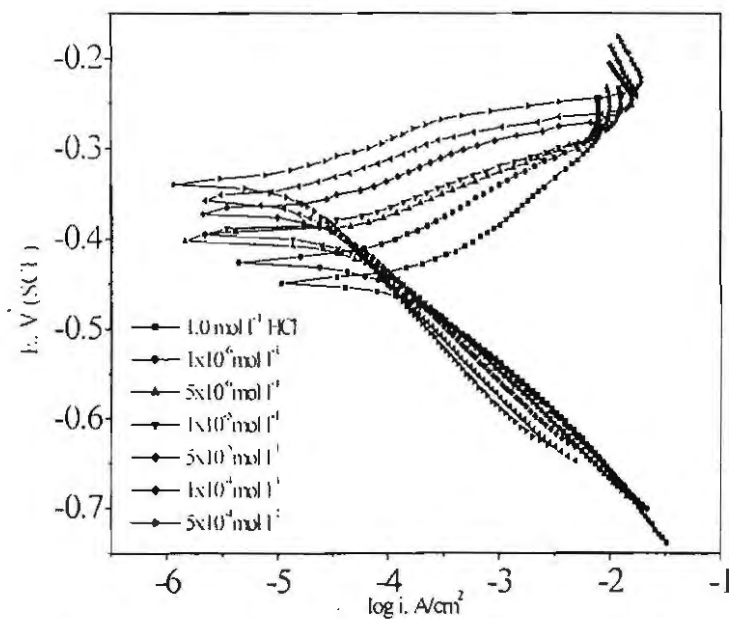


Fig.6. Potentiodynamic polarization curves for the corrosion of stainless steel type 304 in 1.0 mol l⁻¹ HCl in absence and presence of different concentrations of inhibitor (C) at 25°C.

Table (4): Effect of concentrations of inhibitors A, B and C on the electrochemical parameters of stainless steel type 304 in 1.0 mol l⁻¹ HCl at 25°C.

Inhibitor	[Inh.] mol l ⁻¹	-E _{OC} mV	-E _{corr} mV	i _{corr} , μA m ⁻²	-β _c , mVdec ⁻¹	β _a , mV dec ⁻¹	R _p ohm cm	C.R. mm yr ⁻¹
A	1.0M HCl	437.5	449	199.1	126.4	94.0	117.6	2.311
	1×10 ⁻⁶	425.3	446	193.5	121.4	82.3	110.1	2.246
	5×10 ⁻⁶	400.6	427	104.5	117.5	68.1	179.1	1.213
	1×10 ⁻⁵	392.5	423	81.09	115.1	63.1	218.4	0.941
	5×10 ⁻⁵	373.6	392	44.85	114.4	53.1	351.3	0.521
	1×10 ⁻⁴	367.5	377	20.88	107.2	47.6	685.4	0.242
	5×10 ⁻⁴	329.4	370	18.86	106.7	46.2	742.3	0.219
B	1×10 ⁻⁶	423.9	436	115.9	117.7	76.7	174.0	1.345
	5×10 ⁻⁶	384.5	427	96.57	116.3	75.9	206.5	1.121
	1×10 ⁻⁵	388.6	414	51.38	110.0	62.5	336.8	0.596
	5×10 ⁻⁵	330.8	392	25.44	102.0	52.7	593.5	0.295
	1×10 ⁻⁴	362.6	371	22.99	114.5	50.3	660.0	0.267
	5×10 ⁻⁴	356.2	364	19.27	113.6	46.8	747.5	0.224
C	1×10 ⁻⁶	400.2	425	83.21	111.4	76.8	237.2	0.966
	5×10 ⁻⁶	386.1	402	49.00	113.5	57.5	338.0	0.569
	1×10 ⁻⁵	374.5	392.6	25.53	102.0	44.9	530.2	0.296
	5×10 ⁻⁵	331.2	370	18.36	107.9	43.7	735.9	0.213
	1×10 ⁻⁴	346.6	355	15.08	119.4	46.1	957.6	0.175
	5×10 ⁻⁴	328.7	338	12.64	129.8	49.4	1230.0	0.147

$$\theta = [1 - (R_p / R_{p_{inh}})] \quad (15)$$

where i_{corr} and $i_{corr(inh)}$ are the corrosion current densities of uninhibited and inhibited solutions, respectively, R_p and $R_{p_{inh}}$ are the polarization resistance of uninhibited and inhibited experiments, respectively. The percentage of inhibition efficiency, IE% at each concentration was calculated using the equation:

$$IE\% = (1 - R_p / R_{p_{inh}}) \times 100 \quad (16)$$

The percentage inhibition efficiencies (IE% calculated from i_{corr} and IE% calculated from R_p) of the investigated compounds are given in Table (5). An inspection of the results obtained from Table (5, 6) reveals that, the presence of different concentrations of the additive compounds reduce the anodic and cathodic current densities, and the suppression in current increases as the inhibitor concentration increases, this indicate that the inhibiting effects of the investigated compounds.

Table (5): The inhibition efficiencies of different concentrations of inhibitors A, B and C for the corrosion of stainless steel type 304 in 1.0 mol l⁻¹ HCl at 25°C as obtained from potentiodynamic polarization measurements.

Inhibitor Conc. mol l ⁻¹	Compound (A)		Compound (B)		Compound (C)	
	IE%, i_{corr}	IE%, R_p	IE%, i_{corr}	IE%, R_p	IE%, i_{corr}	IE%, R_p
1x10 ⁻⁴	2.8	-6.8	41.8	32.4	58.2	50.4
5x10 ⁻⁴	47.5	34.3	51.5	43.1	75.4	65.2
1x10 ⁻³	59.3	46.2	74.2	65.1	87.2	77.8
5x10 ⁻³	77.5	66.5	80.6	72.4	90.8	84.0
1x10 ⁻¹	89.5	82.8	88.5	82.2	92.4	87.7
5x10 ⁻¹	90.5	84.2	90.3	84.3	93.7	90.4

The slight shifts of E_{corr} values towards less negative direction are found in the presence of various concentrations of these compounds in 1.0 M HCl. Generally, increase in inhibitor concentration shifts corrosion potential to less negative values. This can be explained by a small domination of the anodic reaction inhibition [Stupnisek-Lisac *et al.*, (2002)]. However, these compounds influence the cathodic reaction at potentials greater than the desorption potential. This indicates that these compounds exhibit both anodic and cathodic inhibition effects. Small changes in potentials can be a result of the competition of the anodic and the cathodic inhibiting reactions, and of the metal surface condition [g]. Meanwhile, from Table 4, the slopes of the cathodic Tafel lines (β_c) and anodic Tafel lines (β_a) are observed to change with addition of inhibitors,

which indicates influence on both the cathodic and anodic reactions, the cathodic curves are more affected. Thus these inhibitors act as mixed type inhibitors for stainless steel in 1.0 M HCl. The %IE was found to increase with increasing the inhibitor concentration. The inhibition achieved by these compounds decreases in the following order:

Compound C > Compound B > Compound A

Table (6): Effect of addition of different concentrations of KI with 1×10^{-6} mol l^{-1} of inhibitors A, B and C on the electrochemical parameters of stainless steel type 304 in 1.0 mol l^{-1} HCl at 25°C.

Inhibitor	Conc of KI (mol l^{-1})	$-E_{oc}$ mV	$-E_{corr}$ mV	i_{corr} μA cm^{-2}	$-\beta_c$ mV dec^{-1}	β_a mV dec^{-1}	Rp ohm cm	C.R. mm yr^{-1}
A	—	425.3	446.3	193.5	121	82	110.1	2.246
	1×10^{-1}	347.3	380.9	77.66	119	90	288.7	0.902
	1×10^{-2}	307.6	345.2	23.61	116	77	853.7	0.274
	1×10^{-2}	243.9	316.9	17.12	128	82	1263.0	0.199
B	—	423.9	436.0	115.9	118	111	174.0	1.345
	1×10^{-4}	353.9	380.5	49.13	110	82	380.1	0.570
	1×10^{-3}	312.7	346.7	21.44	118	85	891.2	0.249
	1×10^{-2}	242.8	318.1	16.24	127	120	1309.0	0.188
C	—	400.2	424.8	83.21	111	77	237.2	0.966
	1×10^{-1}	357.8	382.8	43.68	111	62	395.3	0.507
	1×10^{-1}	317.3	348.2	17.50	115	55	924.4	0.203
	1×10^{-2}	276.2	322.3	14.63	128	67	1305.0	0.170

3.2.1. Synergistic effect

The increase in inhibition efficiency of organic compounds in the presence of some anions has been observed by several investigators [Umoren *et al.*, (2006); Umoren & Ebenso (2007); Oguzic & Ebenso (2006) and Gomma (1998)] and was ascribed to synergistic effect. Trials to enhance the performance of the used inhibitors by addition of KI were carried out using potentiodynamic measurements. Figs.7. shows potentiodynamic polarization curves for stainless steel type 304 in 1.0M HCl in the absence and presence of 1×10^{-6} M of compound C without and

with different concentrations (1×10^{-4} , 1×10^{-3} , $1 \times 10^{-2} \text{M}$) of KI at 25°C . The obtained electrochemical values (E_{OC} , E_{corr} , i_{corr} , β_c , β_a and R_p) are shown in Table (6). The calculated inhibition efficiency values are shown in Table (7). Results shown in the Tables revealed that the presence of different concentrations of KI enhances the reduction of i_{corr} values for stainless steel in 1.0M HCl and the reduction in the rate increases with increasing the concentration of KI indicating that addition of KI increases the inhibiting action of the investigated inhibitors.

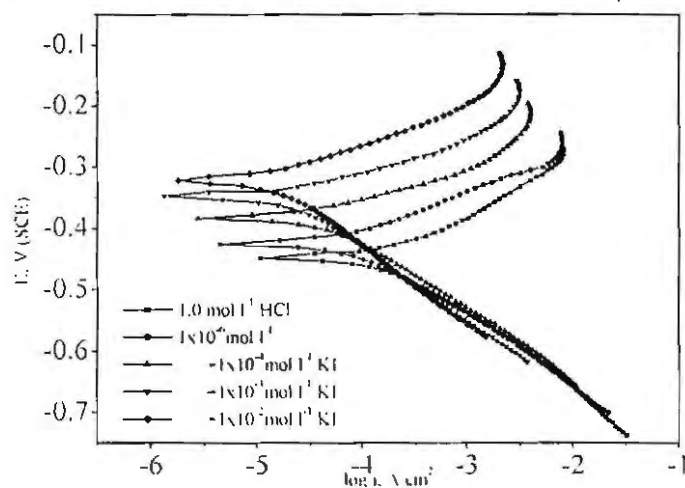


Fig. 7 Potentiodynamic polarization curves of stainless steel type 304 in 1.0 mol l^{-1} HCl in absence and presence of $1 \times 10^{-4} \text{ mol l}^{-1}$ of inhibitor (C) and different concentration of KI at 25°C

The order of increasing inhibition efficiency for the investigated inhibitors in the presence of $1 \times 10^{-2} \text{M}$ KI and in case of constant concentration from the investigated inhibitors with different concentration of KI for stainless steel in 1.0M HCl is as follow:
Compound C > compound B > compound A.

Table (7): Effect of addition of different concentrations of KI on the inhibition efficiency of 1×10^{-6} mol l⁻¹ of inhibitors A, B and C for the corrosion of stainless steel type 304 in 1.0 mol l⁻¹ HCl at 25°C.

Conc of KI (mol l ⁻¹)	304SS					
	Compound (A)		Compound (B)		Compound (C)	
	IE%, i_{corr}	IE%, R_p	IE%, i_{corr}	IE%, R_p	IE%, i_{corr}	IE%, R_p
—	2.8	-6.8	41.8	32.4	58.2	50.4
1×10^{-4}	61.0	59.3	75.3	69.1	78.1	70.3
1×10^{-3}	88.1	86.2	89.2	86.8	91.2	87.3
1×10^{-2}	91.4	90.7	91.8	91.0	92.7	91.0

3.2.2. Anodic polarization measurements (pitting corrosion)

NaCl is one of the most common materials used in pitting corrosion for some metals such as stainless steel. The polarization curves for stainless steel type 304 in different concentrations of NaCl solution are shown in Fig. 8. The scans have the same general features and characterized by the appearance of active, passive and transpassive regions before oxygen evolution. The passivation current (i_{pass}) decreases over extending a wide range of potential due to formation of the passive layer on the Stanly surface. After the corrosion potential (zero current), the anodic current density starts to increase to form the active region. The increase of the potential in the positive direction leads to increasing of the anodic current, which corresponds to the oxidation of iron to iron ions. With increasing the potential a passive film [Fe(OH)₂, Fe₃O₄ and/or Fe₂O₃] can form [Pourbaix (1974)].

The addition of different concentrations from compound (C) to 0.1M NaCl solution for the corrosion of stainless steel type 304 increases the breakdown potential towards more positive values (Figs. 9), i.e. inhibits pitting corrosion of the stainless steels. Fig. 10. shows the relation between E_{pit} and the inhibitors concentrations for 304 stainless steel, a straight line obtained according to the following equation:

$$E_{pit} = a' + b' \log [\text{inh.}] \quad (17)$$

Symbols a' and b' are constants. The increase of the inhibitors concentration increases the pitting potential to more positive values, i.e. decreases the pitting corrosion. The adsorption of the inhibitors on the

stainless steels surfaces can prevent the adsorption of Cl ion (which is responsible for pitting corrosion).

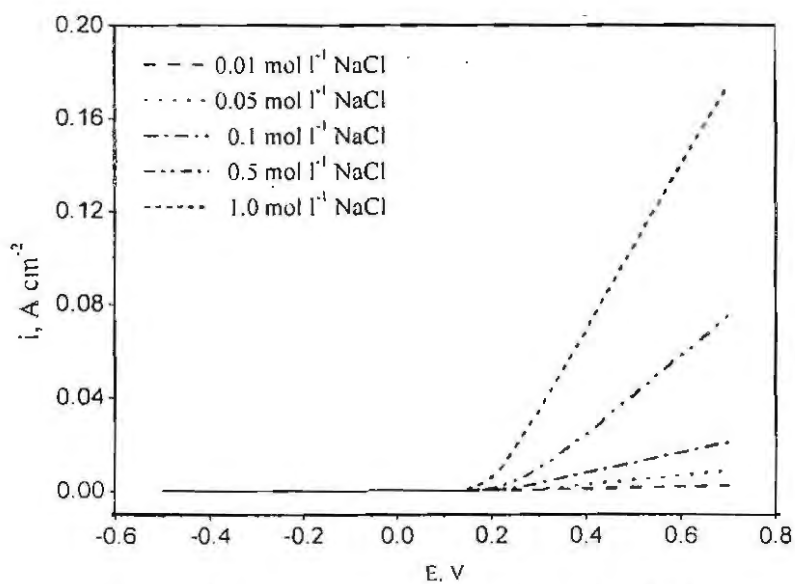


Fig. 8. Anodic Potentiodynamic curves for stainless steel type 304 in presence of different concentrations of NaCl

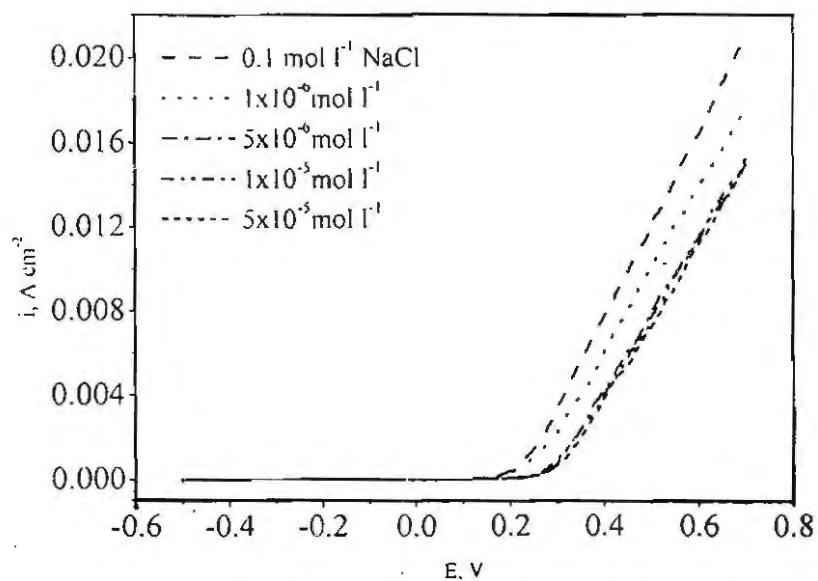


Fig. 9. Anodic Potentiodynamic curves for stainless steel type 304 in 0.1 mol l⁻¹ NaCl in the absence and presence of different concs. of compound (C).

3.3. Electrochemical Impedance Spectroscopy (EIS)

The corrosion of stainless steel type 304 in 1 M HCl in the presence of investigated compounds was investigated by EIS method at 25°C after 20 min immersion. Nyquist and Bode plots in the absence and presence of investigated compound (C) are presented in Figs. 11 and 12. Similar curves were obtained for other inhibitors. It is apparent that all Nyquist plots show a single capacitive loop, both in uninhibited and inhibited solutions. The impedance data of stainless steel in 1.0 M HCl are analyzed in terms of an equivalent circuit model (Fig. 13) which includes the solution resistance R_s or R_Ω and the double layer capacitance C_{dl} which is placed in parallel to the charge transfer resistance R_{ct} [Sekine *et al.*, (1992)] due to the charge transfer reaction. For the Nyquist plots it's obvious that low frequency data are on the right side of the plot and higher frequencies are on the left. This is true for EIS data where impedance usually falls as frequency rises (this is not true of all circuits).

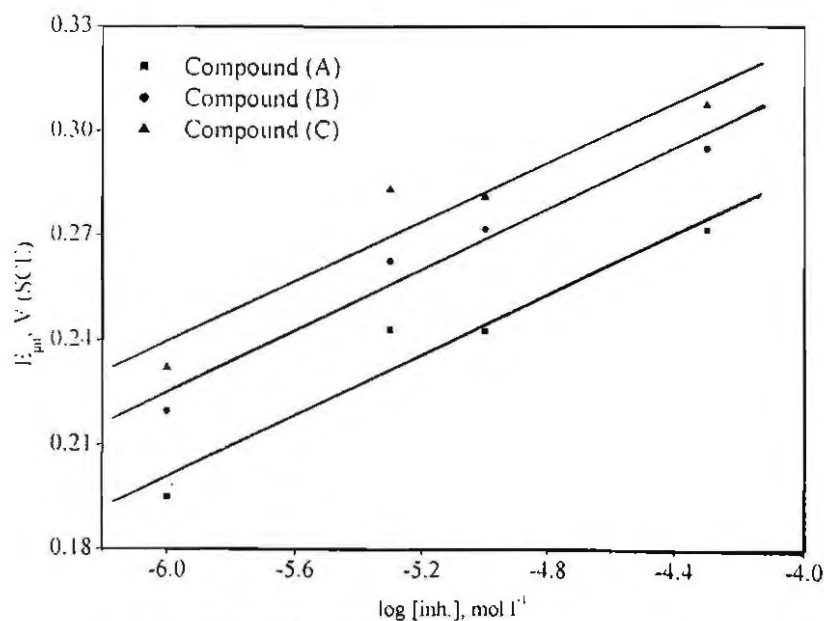


Fig. 10 Pitting potential (E_{pit}) as a function of inhibitors A, B and C concentration for stainless steel type 304 in 0.1 mol l⁻¹ NaCl.

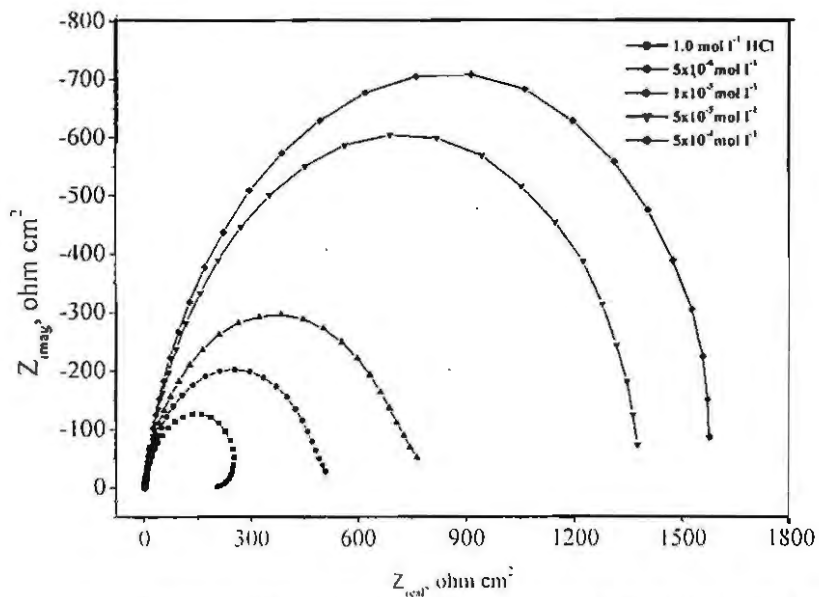


Fig. 11. The Nyquist plots for the corrosion of stainless steel type 304 in 1.0 mol l⁻¹ HCl in the absence and presence of different concs. of inhibitor (C) at 25°C.

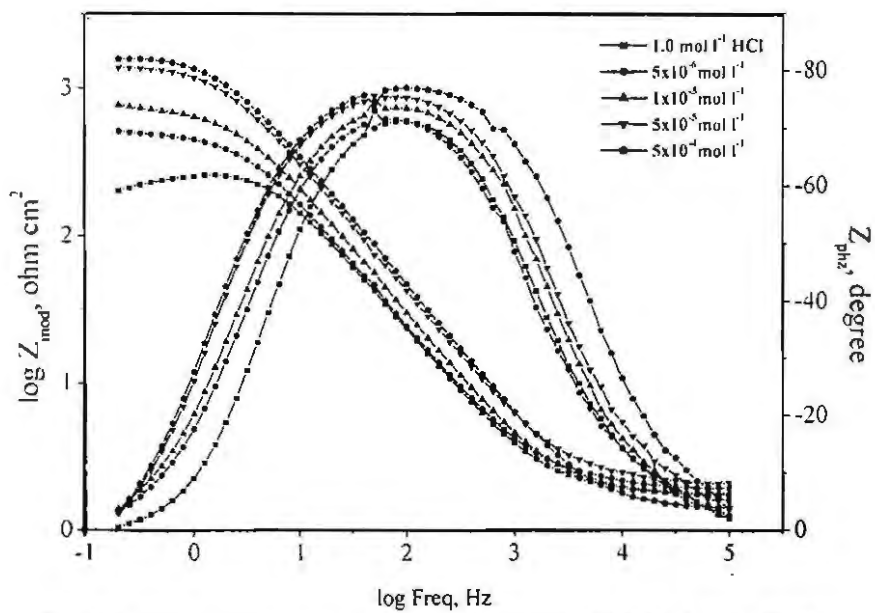


Fig. 12. The Bode plots for the corrosion of stainless steel type 304 in 1.0 mol l⁻¹ HCl in the absence and presence of different concentrations of inhibitor (C) at 25°C.

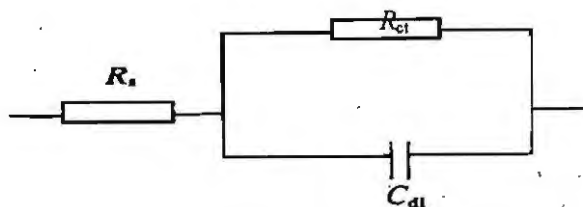


Fig.(13): The equivalent circuit model used to fit the experimental result.

The capacity of double layer (C_{dl}) can be calculated from the following equation

$$C_{dl} = \frac{1}{2\pi f_{max} R_{ct}} \quad (18)$$

where f_{max} is maximum frequency.

The parameters obtained from impedance measurements are given in Table (8). It can be seen from Table 8 that the values of charge transfer resistance increase with inhibitor concentration [Larabi *et al.*, (2006)]. In the case of impedance studies, IE% increases with inhibitor concentration in the presence of investigated inhibitors and the IE% of these investigated inhibitors is as follows: Compound C > compound B > compound A. The impedance study confirms the inhibiting characters of these compounds obtained with weight loss and potentiodynamic polarization methods. It is also noted that the (C_{dl}) values tend to decrease when the concentration of these compounds increases. This decrease in (C_{dl}), which can result from a decrease in local dielectric constant and/or an increase in the thickness of the electrical double layer, suggests that these compounds molecules function by adsorption at the metal/solution interface [Lagrence *et al.*, (2002)].

The inhibiting effect of these compounds can be attributed to their parallel adsorption at the metal solution interface. The parallel adsorption is owing to the presence of one or more active center for adsorption. The chemisorption takes place by the formation of a chemical bond between the metal and the adsorbed molecule. Chemisorption involves charge or charge transfer from inhibitor molecule to the metal surface forming coordinate type bond [Khamis *et al.*, (1991)].

Table (8): Electrochemical kinetic parameters obtained by EIS technique for the corrosion of stainless steel type 304 in 1.0 mol l⁻¹ HCl at different concentrations of inhibitors A, B and C at 25°C.

Inhibitor	Conc (mol l ⁻¹)	C _{dl} (μF cm ⁻²)	-Phase (degree)	R _p (ohm)	θ	IE%
A	1.0 mol l ⁻¹ HCl	71.35	71.3	234.6	----	----
	5x10 ⁻⁶	73.07	72.0	333.5	0.297	29.7
	1x10 ⁻⁵	71.04	71.4	349.8	0.329	32.9
	5x10 ⁻⁵	55.18	73.3	683.1	0.657	65.7
	5x10 ⁻¹	44.68	75.0	991.5	0.763	76.3
B	5x10 ⁻⁶	72.99	70.1	417.5	0.438	43.8
	1x10 ⁻⁵	68.24	70.3	425.9	0.449	44.9
	5x10 ⁻⁵	46.55	75.2	779.3	0.699	69.9
	5x10 ⁻¹	38.94	76.8	965.9	0.757	75.7
C	5x10 ⁻⁶	72.06	71.6	430.6	0.455	45.5
	1x10 ⁻⁵	58.12	73.5	628.0	0.626	62.6
	5x10 ⁻⁵	41.81	75.2	1216.0	0.807	80.7
	5x10 ⁻¹	36.68	77.0	1404.0	0.833	83.3

3.4. Mechanism of inhibition

Many organic compounds with at least one polar unit containing atoms of nitrogen, sulfur oxygen are known to function as corrosion inhibitors. The polar unit is regarded as the reaction centre for the adsorption process. In such a case the adsorption bond strength is determined by the electron density on the atom acting as the reaction centre and by polarisability of the unit. Thus, polar organic compounds acting as corrosion inhibitors are adsorbed on the surface of the metal, forming a charge transfer complex between their polar atoms and the metal. The size, shape and orientation of the molecule and the electronic charge on the molecule determine the degree of adsorption and hence the effectiveness of the inhibitor.

The investigated inhibitors confer high protection to stainless steels corrosion in 1.0M HCl and function through adsorption on the metal surface following Langmuir isotherm. The obtained results by

weight loss, potentiodynamic polarization and electrochemical impedance spectroscopy (EIS) techniques indicate that the extent of corrosion inhibition of the investigated compounds followed the following order: $C > B > A$. It can be explained on the basis of adsorption. It is apparent from the molecular structure that, these compounds can be adsorbed on the metal surface through the lone pair of electrons of oxygen and/or nitrogen and/or sulfur atoms and delocalized π -electrons of benzene ring. The difference in the inhibition efficiencies can be explained on the basis of the type and the number of hetero atoms in the cavity of these compounds. Also the inhibition efficiency values can be explained on the basis of the molecular weight, compound (C) exhibits excellent inhibition efficiency due to its molecular weight (667.65) that may facilitate better surface coverage. Compound (B) comes after compound (C) in inhibition efficiency because it has lesser molecular weight (546.58). Compound (A) has the lowest inhibition efficiency; this is because it has the lowest molecular weight (517.02) and has no aromatic ring.

4. CONCLUSIONS

3-thiazinonyl-bicyclo [4.2.0]octene-carboxylate derivatives have proved to be environmentally-friendly corrosion inhibitors for corrosion of stainless steel type 304 in 1.0 M HCl solution. These inhibitors act as mixed type inhibitors but the anode is more polarized when an external current was applied and IE% was found to increase by increasing the inhibitor concentration and decrease with rising the temperature. The IE% obtained from electrochemical impedance spectroscopy and potentiodynamic polarization measurements show good agreement with those obtained from weight loss experiments.

The inhibition of stainless steel type 304 in 1.0M HCl solution was found to obey Langmuir adsorption isotherm. The thermodynamic values obtained from this study indicate that the presence of the inhibitors increases the activation energy and the negative values of ΔG_{ads}^0 indicate spontaneous adsorption of the inhibitors on the surface of the steel.

REFERENCES

- Szypowski, A.J. *Br. Corros. J.* 37 (2002) 141.
- Quraishi, M.A. Ansari, F.A. Jamal, D. *Mater. Chem. Phys.* 77 (2003) 687.
- Elachouri, M. Hajji, M.S. Kertit, S. Essassi, E.M. Salem M. and Coudert, R. *Corros.Sci.*, 37 (1995) 381.
- Merari, B. Elattar, H. Traisnel, M. Bentiss F. and Larenee, M. *Corros.Sci.*, 40 (1998) 391.
- Bentiss, F. Traisnel, M. Lagrenee, M. *Corros.Sci.*, 42 (2000) 127.
- Elkadi, L. Mernari, B. Traisnel, M. Bentiss F. and Lagrenee, M. *Corros.Sci.*, 42 (2000) 703.
- Walker, R. *corros.Sci.*, 31 (1975) 97.
- Bentiss, F. Lagrenee, M. Traisnel M. and Lornez. *J.C. Corros.Sci.*, 41 (1999) 789.
- El-Kanouni, A. Kertti, S. Srhiri. A. Bachir, K. *Bull. Electrochem.* 12 (1996) 517.
- Talati. J.D. and Modi. R.M. *Trans.SEAST*, 11 (1986) 259.
- Szklarska-Smialowska: *Z. Electrochemical and Optical Techniques for the Study of Metallic Corrosion*, Kluwer Academic, the Netherlands; (1991) 545.
- Langmuir, I. *Amer. J. Chem.Soc.*, 39 (1947) 1848.
- Khamis, E. *Corrosion.* 46 (1990) 476.
- El-Awady Y.A. and Ahmed, A.I. *Ind. J. Chem.*, 24A (1985) 601.
- Putilova, I.K. Balizen, S.A. Barasanik, Y.P. *Metallic corrosion inhibitors*, Pergamon Press. Oxford, 1960, P. 30.
- Laque F. L. and Gapson; H. R. *Corrosion resistance of metals and alloys*; 2nd ed.. Reinhold publishing corporation, New York, (1963).

Banerjee, S. N. "An introduction to science of corrosion and its inhibition" Ox-anion Press, Pvt Ltd., New Delhi, (1985).

Zhao T.P. and Mu, G.N. *Corros.Sci.*, 41 (1999) 1937.

Fouda, A. S. Mostafa, H. A. El-Taib F. and El-Ewady G. Y. *Corros. Sci.*, 47(2005)1988-2004.

Fouda, A.S. Al-Sawary. A.A. Ahmed, F.Sh. El-Abbasy; H.M. *Corros. Sci.*; (2009) in press.

Riggs L. and Hurd: R. M. *Corrosion*; 23 (1967) 252.

Gomma M. K. and Wahdan: M. H. *Mater. Chem. Phys.* 39 (1995) 209.

Ammar, I. A. Darwish. S. *Corros. Sci.* 7 (1967) 679.

Fisher, H. *Ann. Univ. Ferrera. Sez. 3 (Suppl. 3)* (1960) 1.

Stupnisek-Lisac. E. Gazivoda A. and Madzarac, M. *Electrochim.Acta.* J.47 (2002),4189.

Umoren. S.A. Ogbobe O. and Ebenso. E.E. *Trans SAEST* 41 (2006) 74

Umoren S.A. and Ebenso. E.E. *Mater. Chem. Phys.*: 106 (2007) 387.

Oguzie E.E. and Ebenso. E.E. *Pigment Resin Technol.*: 35 (2006) 30.

Gomma; G.K. *Mater. Chem. Phys.*: 55 (1998) 241.

Pourbaix: M. "Atlas of Electrochemical Equilibria in Aqueous Solutions". National Association of Corrosion Engineering, second ed. (English). Houston. Texas. USA. (1974).

Sekine, I. Sabongi, M. Hagiuda. H. Oshibe. T. Yuasa, M. Imahc, T. Shibata, Y. and Wake: T. *Electrochem. J. Soc.*: 139 (1992) 3167.

Larabi, L. Benali, O. Mekelleche S.M. and Harek. Y. *J.Appl.Surf.Sci.*, 253 (2006) 1371.

Lagrennee, M. Mernari. B. Bouanis, B. Traisnel M. and Bentiss, F. *Corros.Sci.*, 44 (2002) 573.

Khamis, E. Bellucci, F. Latahision, R.M. El-Ashry, E.Sh. *Corrosion* 47 (9) (1991) 667.

بعض مشتقات 3-ثيازينونيل-بايسيكلو [4.2.0] اوكتين كاربوكسيليت كمثبطات صديقة للبيئة لتآكل الصلب المقاوم 304 في محلول 1 مولر HCl.

عبد العزيز السيد فوده - هانم عبد الرسول مصطفى
- ونام ابو المعاطى - هناء العباسى

تم دراسة التأثير المثبط لمشتقات 3-ثيازينونيل-بايسيكلو [4.2.0] اوكتين كاربوكسيليت على تآكل الصلب المقاوم 304 في 1 مول حمض الهيدروكلوريك بطريقة فقد الوزن وطريقة الاستقطاب البتشدوديناميكي وطريقة المعاوقة الكهربية وقد وجد أن كفاءة التثبيط تزداد بزيادة التركيز وتقل بزيادة درجة الحرارة وتم حساب بعض السوال الترموديناميكية لعملية التنشيط والادمصاص وقد وجد أن هذه المشتقات تعمل كمثبطات مختلطة وتتمص على سطح الصلب المقاوم تابعة أيزوثرم لانجمير وقد وجد أن كفاءة التثبيط تزداد بزيادة اضافة بعض الانيونات ووجد أن النتائج المتحصل عليها من الطرق الثلاثة متطابقة تماما.